https://dspace.org/

Quartz and feldsparblended clay composites for thermal and structural applications

C.P Egole; R.O Medupin; G.C Nzebuka; N.A Nomnodum; U.P Ochieze ...

https://hdl.handle.net/10539/39832
SCOPUS

Downloaded from a DSpace repository. https://dspace.org/

Results in Materials 23 (2024) 100584

Contents lists available at ScienceDirect

Results in Materials

journal homepage: www.sciencedirect.com/journal/results-in-materials

Quartz and feldspar-blended clay composites for thermal and structural applications

Chijioke P. Egole [a], Rasaq O. Medupin [a], Gaius C. Nzebuka [b], Nnamdi A. Nnodum [a], Ugochukwu P. Ochieze [a], Orevaoghene Eterigho-Ikelegbe [c], Uwemedimo N. Wilson [d], Kelvin O. Yoro [e,*]

[a] Department of Materials and Metallurgical Engineering, Federal University of Technology, 460114, Owerri, Nigeria
[b] Department of Mechatronics Engineering, Federal University of Technology, 460114, Owerri, Nigeria
[c] Clean Coal Technology Research Group, School of Chemical and Metallurgical Engineering, Faculty of Engineering and the Built Environment, University of the Witwatersrand, Private Bag X3, Wits, 2050, Johannesburg, South Africa
[d] Department of Civil Engineering, Nigerian Defence Academy, P.M.B, 2109, Kaduna, Nigeria
[e] Energy Technologies Area, Lawrence Berkeley National Laboratory, 1 Cyclotron Road, Berkeley, CA, 94720, United States

ARTICLE INFO

Keywords:
Raw clay
Fired clay
Green composites
Sustainable development
Thermogravimetric analysis

ABSTRACT

In this study, some selected clay samples were beneficiated and blended with quartz and feldspar in various proportions to develop composites with good thermal and structural performance for sustainable development. X-ray fluorescence (XRF) analysis affirms the aluminosilicate nature of the clay samples and other trace oxides. The pore volume of the fired bulk composites disappears at 1200 °C leading to a decline in apparent density, apparent porosity, and water absorption. Furthermore, this study revealed that at the same temperature, the bulk density (1.69, g/cm^3, 1.78, g/cm^3, 1.78 g/cm^3), modulus of rupture (33.2 kg/cm^3, 39.34 kg/cm^3, 38.88 kg/cm^3), and total shrinkage (23.6 %, 22.3 %, 20.6 %) were maximum. Additionally, the results showed that the relative plasticity of the clay samples improved with the addition of feldspar and quartz from 1.27 to 1.33 and 1.35 for the fired composites (BO1: 50 % clay, 30 % feldspar, 20 % quartz, and CO1: 50 % clay, 25 % feldspar, 25 % quartz), respectively. Results obtained from thermogravimetric analysis (TGA) and differential scanning calorimetry (DSC) analysis confirmed the clay samples to be thermally stable. The X-ray diffraction (XRD) patterns of all the fired composites showed major peaks, with quartz content being the highest at 27.5° (2θ) angle, albite presenting the lowest non-clay mineral content. Based on the analyses conducted in this study, it could be inferred that the clay sample is suitable for thermal insulation and structural applications.

1. Introduction

Harnessing the abundant clay deposits on the landscape of many developing countries across the world could catalyze the emergence of sustainable manufacturing industries [1,2]. In the past, Mucke et al. [3] reported that virtually all the regions of the world are naturally endowed with enormous deposits of clay. However, Dansarai et al. [4] argued that new applications of the identified clay deposits could bring about economic prosperity globally. According to Ugwuoke and Amalu [5], clay is a mineral on the surface of the earth that occurs as a result of digenetic and hydrothermal alteration of rocks. This non-metallic material possesses massive heat capacity and can withstand high temperatures and pressures, thermal shock, chemical attacks, and heavy loads at elevated temperatures [6]. Significantly, the clay material can retain its shape, strength, chemical, and dimensional integrity at high temperatures. These potentials make materials that would be subjected to these conditions, refractory materials, for instance, very useful in the production of devices and equipment like furnaces, incinerators, crucibles, electrical insulators, and other metallurgical furnace linings where resistance to high temperatures is of the essence. These devices are significant in the processing of raw materials into finished goods in manufacturing industries. Clay materials occur geologically as particles with phyllosilicates or sheet structures. They have diameters ranging from less than 2 μm to 100 μm and are most naturally in solids, sediments, sedimentary rocks, hydrothermal deposits, and abundantly in every part of Nigeria.

* Corresponding author.
E-mail address: kelvin.yoroo@gmail.com (K.O. Yoro).

https://doi.org/10.1016/j.rinma.2024.100584
Received 12 March 2024; Received in revised form 3 May 2024; Accepted 4 June 2024
Available online 5 June 2024
2590-048X/© 2024 The Authors. Published by Elsevier B.V. This is an open access article under the CC BY-NC-ND license (http://creativecommons.org/licenses/by-nc-nd/4.0/).

Several investigations have been reported on several clay deposits with remarkable success. For example, Amkpa et al. [7] studied the Alkaleri clay deposit in Bauchi State, Northeastern Nigeria to verify the suitability of the high silica and alumina deposits for refractory applications. Conclusion made centers on the improvement of the cold crushing strength, firing shrinkage, and bulk density because of mechanical activation through the sintering process. Findings made were comparable to that of Ojonimi et al. [8], which investigated the Egbahieme clay deposit in Kogi State, North Central Nigeria. Both deposits share similar properties, including the unavoidable inclusion of impurities. In a similar study, Ajala & Badarulzaman [9] isolated the Aloji clay deposit from a site in Kogi State for investigative studies. Findings from the investigation indicated that the Aloji fireclay possesses sufficient attributes for application in foundry technology as refractory fireclay bricks. Similarly, Okpanachi et al. [10] reported on Kaduna, Tagwai, and Gbakoita clay deposits located in Niger State, Nigeria. While Kaduna clay was found physically suitable for both fire and siliceous fire clay, Tagwai clay could only withstand 1200 °C maximum due to its low refractoriness, thermal shock resistance, and bulk density, despite its good linear shrinkage, apparent porosity, and cold crushing strength. Of the three clay deposits, Gbakoita clay was found to perform poorly as a refractory material, falling below standard specifications for the application. Each of these independent studies established the fact that Nigeria's clay deposits are rich in silica and alumina and satisfy the physical, mechanical, and thermal requirements for many applications. Another area of application of clay that dates back to the pre-colonial era is in building materials, especially reinforced bricks and blocks. More research efforts have to be dedicated to this area because of the huge housing deficit in Nigeria in the face of the rising cost of conventional cement, a major component of building blocks.

Clay minerals are special materials whose properties are largely influenced by their geographical location, relative humidity, chemical composition, and processing parameters. The thermal and chemical stability of clays has endeared them to applications in building services, heat treatments, and electrical power infrastructure. The type of reaction that will take place during the thermal processing of clays depends on the specific minerals that make up the clay [11]. Recent studies on chemical, phase, and thermal analyses to determine the composition of the raw materials and production technology have been presented by Kostova et al. [12]. Their results suggest that clay type cannot be determined by one method alone. Therefore, a combination of different methods is critical for the accurate identification of mineralogical components of clay deposits and their suitability for various applications.

The primary contributions of this study is the exploration of the synergistic effects achieved by blending quartz and feldspar with clay. This combination harnesses the unique properties of each component to create composites with enhanced thermal and structural characteristics. Furthermore, this study was designed to investigate selected clay samples towards developing products from clay deposits, with many of them seeking to compare the properties of products made from them across different regions of the world. Through meticulous synthesis methods, characterization, and applications-driven research, these composites are poised to revolutionize industries ranging from construction to manufacturing. Embracing the potential of these innovative materials is essential for addressing global challenges and advancing towards a more sustainable future. Overall, the novelty and major contribution of this study lies in its exploration of the synergistic properties of quartz and feldspar-blended clay composites, their tailored applications across various sectors, and their role in advancing sustainability as well as efficiency in materials science and engineering.

2. Materials and methods

2.1. Materials

The major raw material (clay sample) used in this study was mined from Okitipupa, South West Nigeria. This area falls within Latitude 6°36′ 28.31″ N and Longitude 4°46′ 27.75″ E on the globe. The geographical location is rich in several grades of mineral resources, including clay minerals, that met the specifications of numerous manufacturing and service sectors. The clay additive (processed quartz) was sourced from Enugu State, in southeastern Nigeria. While beneficiated feldspar was obtained from Abeokuta, in the southwest of Nigeria.

2.2. Experimental method

The clay sample from the collection site was dried, crushed, and screened, then packaged using the procedure described in Shan et al. [13]. A 3 kg measure of the clay was weighed and soaked in 10 L of water. This was then mixed for 15 min using an electrically powered mechanical mixer, within which the lighter impurities were expected to separate themselves from the clay and float while heavier impurities settled at the bottom of the containing vessel. The mixture was then allowed to settle for 3 days. The resulting mix was decanted and dewatered, dried further in an electric oven, and passed through sieves of 425 μm and 180 μm meshes. Subsequently, the raw clay was blended with quartz and feldspar in different proportions to yield various samples, as indicated in Table 1.

The beneficiated clay sample was then mixed with water in a ratio of 6:1 (sample to water) to make it malleable. The malleable mixture was then used to produce 10.0 mm diameter by 65.0 mm height cylindrical test specimens and 70.0 mm length × 25.0 mm width × 15.0 mm height rectangular test specimens in a lubricated metallic mold. The samples were left to harden under atmospheric conditions for 168 h for slow but steady drying, followed by oven-drying at 110 °C for 4 h to remove moisture that could not be removed by natural drying, thus forming the raw clay (AO1) and green/dried composites (BO1 and CO1) which were subsequently subjected to higher temperature at 1100 °C during firing exercise in the furnace.

2.3. Evaluation of the raw clay and the composites

X-ray fluorescence was carried out to determine the elemental composition of the raw clay sample using X-ray diffraction equipment (Model Phillips PW-1800). A water absorption test was performed on the fired raw clay and the blended clay composites following the procedure described in Medupin et al. [14]to study the samples' durability and behavior in weathering. The moisture content of the clay samples was determined after drying in the oven at 110 °C for 24 h, according to the method reported by Shuaib-Babata et al. [1]. The calculation of apparent porosity, that is the relationship of the volume of the open pores in the specimen to its exterior volume, was done according to the method described by Chindaprasirt [15], and Aluko & Ikubuwaje [16]. The bulk density of the specimen expressed in g/cm^3, which is the quotient of its dry weight, was determined following the method used by Aluko & Ikubuwaje [16]. The flexural strength of the fired clay specimens (modulus of rupture) was determined by a 3-point bend test according to ASTM C133-97 as reported by Samad et al. [17]. Cylindrical geometry samples were used (5.0 mm diameter and 65.0 mm span).

Table 1
Categorization of clay mixtures.

Sample	Clay (g)	Feldspar (g)	Quartz (g)
AO1	100	0	0
BO1	50	30	20
CO1	50	25	25

Both dried and fired clay and their composites were analyzed for modulus of rupture (MOR) using Equation (1).

$$Modulus\ of\ rupture = \frac{3\rho L}{2BH^2} \quad (1)$$

where ρ = load at rupture, L = distance between the center line of the lower bearing edges of the equipment, B = width of composite, and H = thickness of composite (cm).

2.4. Thermal analyses

Thermal analyses are critical analytical techniques for material characterization due to the unique ways in which various materials respond when exposed to varying degrees of thermal energy. In this study, differential scanning calorimetry (DSC), differential thermal analysis (DTA), and thermogravimetric analysis (TGA) were used to evaluate the thermal behavior of the fired clay and fired composites. Combined DSC-DTA was conducted using thermal analysis (TA) equipment ($MDCS_{1600}$-2920). A 6.40 mg measure of each sample was placed on the sample pan while the reference pan was empty. The temperature was then increased from the ambient temperature to 1200 °C at a heating rate of 10 °C/min. Simultaneous thermal conductivity and structural reactions were acquired in the DSC and DTA modes, respectively. The coupled DSC-DTA device was interfaced with a laptop computer, while data acquisition and analysis were done using universal thermal analysis software. Thermogravimetric analysis (TGA) was conducted using another TA instrument (TGA_{1000}-2950). This device makes use of high-melting metal (platinum) as the material for the sample pan. Nitrogen gas was used as the inert gas also to purge the sample inside the heating chamber of the instrument before heating was initiated. The TGA analysis was done at a heating rate of 10 °C/min.

3. Results and discussion

3.1. Chemical analysis of the raw clay and blended clay composites

The geochemical composition of raw clay (AO1)) and blended clay composites (50 % clay, 30 % feldspar, 20 % quartz (BO1), and 50 % clay, 25 % feldspar, and 25 % quartz (CO1)) obtained from XRF is presented in Table 2. The analysis shows that the clay belongs to the fireclay group with silica and alumina compositions in the range of 50–55 % and 15–45 %, respectively [18]. The clay could be considered an aluminosilicate clay, with alumina and silica having the highest percentage of oxides. The higher percentage of SiO_2 for AO1 explains the sandy nature of the clay sample [19], while the low amount of CaO and the absence of MgO in the clay sample is due to the absence of $CaCO_3$ [20].

The value of the Al_2O_3/Fe_2O_3 ratio is said to play a significant role in the determination of the industrial application of fireclay samples. Garcia-Valles et al. [20] reported that if this ratio is less than 5.5, the clay is a high plastic clay, maybe iron-rich, and is suitable for the manufacture of building bricks and yellow-grey tableware. It can be observed also that the inclusion of the additives to the clay increased the SiO_2/Al_2O_3 ratio. For all the samples, the SiO_2/Al_2O_3 ratio is less than 3 %, which signals the presence of high-quality quartz in the studied clay [21]. Additionally, color-forming impurities like Fe_2O_3 and TiO_2 were found to be low and significantly reduced upon the addition of quartz and feldspar to unblended clay. According to Merga et al. [22], low iron content would contribute to the reduction of gas formation at high temperatures when Fe_2O_3 transforms into Fe_3O_4 [23]. In the same vein, the slightly high loss on ignition of 9.7 % can be attributed to the loss of structural hydroxide which occurred during the conversion of kaolinite clay to metakaolinite phase formation at a lower temperature of 500 °C. Therefore, it can be inferred from the mineralogical analysis that the studied clay is suitable for structural application and less prone to porosity-induced failure with the appropriate addition of the additives, quartz, and feldspar.

Table 2
Geochemical composition of the raw clay and blended clay composites.

Predominant oxides	% Distribution of oxides		
	AO1	BO1	CO1
SiO_2	50.701	64.118	64.034
Al_2O_3	33.919	24.484	24.915
Fe_2O_3	1.849	1.207	1.070
TiO_2	2.816	1.903	1.811
CaO	0.128	–	–
P_2O_5	0.432	0.472	0.420
K_2O	0.155	2.932	2.491
Z_rO	0.104	–	–
LOI	9.700	4.600	5.000
SiO_2/Al_2O_3	1.495	2.619	2.570
Al_2O_3/Fe_2O_3	18.345	20.285	23.285

3.2. Physical properties

Fig. 1 shows how the physical properties of the bulk composites of each sample vary when exposed to different temperature conditions in a furnace environment. The apparent density, apparent porosity, and water absorption of the composites decrease with increased firing temperature (See Fig. 1a, b, and c), while the bulk density, modulus of rupture, and shrinkage of the composites increased with increased firing temperature (see Fig. 1d, e, and f). Previous research has demonstrated that the melting of feldspar at temperatures around 1100 °C leads to a liquid/glassy phase that occupies the voids in the microstructure, responsible for densification [24,25]. Merga Tullu et al. [23] reported that feldspar melts as the firing temperature increases and fills up microstructural pores within the composites. Consequently, the pore volume continues to disappear until the temperature reaches 1200 °C. Apparent density, porosity, and water absorption have minimum values while bulk density, modulus of rupture, and total shrinkage have maximum values as shown in Fig. 1. It was also observed that the relative plasticity of the clay samples improved upon the blending of feldspar and quartz, from 1.27 to 1.33 and 1.35 for BO1 and CO1, respectively. This implies that the bulk clay samples become more malleable as their plastic properties are improved, thus providing added benefits during manufacturing activities.

3.3. Thermal analysis, DSC, TGA/DTG

The thermal properties of the unfired clay sample and unfired composites of different compositions containing feldspar and quartz were studied to investigate the effect of the additives on the thermal stability of the materials. Differential scanning calorimetry (DSC) measurements were performed on composites of samples at the heating rate of 10 °C/min, in the temperature range of 300 up to 480 °C, without additional processing before DSC measurement. Temperatures characteristic for thermal transitions of the material were read out from the second heating scan. The heating profiles of raw clay are shown in Fig. 2. The DSC thermograms of clay reinforced with various weight fractions of feldspar and quartz are presented in Figs. 3 and 4. Clear endothermic peaks are observed to be located at the same location in the heating curves. The crystallization of neat clay can be observed at approximately 433 °C, while the onset temperature of degradation and crystallization is observed to have slightly changed. It is obvious that the initial degradation temperature (T_{onset}), which is an indication of the thermal stability of the materials, had the lowest value for the unfired clay. The incorporation of feldspar and quartz into the clay sample shows slight changes in the onset of the composite, as can be seen in the thermograms. Additionally, it can be observed that the change in the percentage of feldspar and quartz components did not affect the thermal stability of the composite clay, not even on the dried clay (Figs. 2–4). This further buttresses the fact that the clay sample is naturally

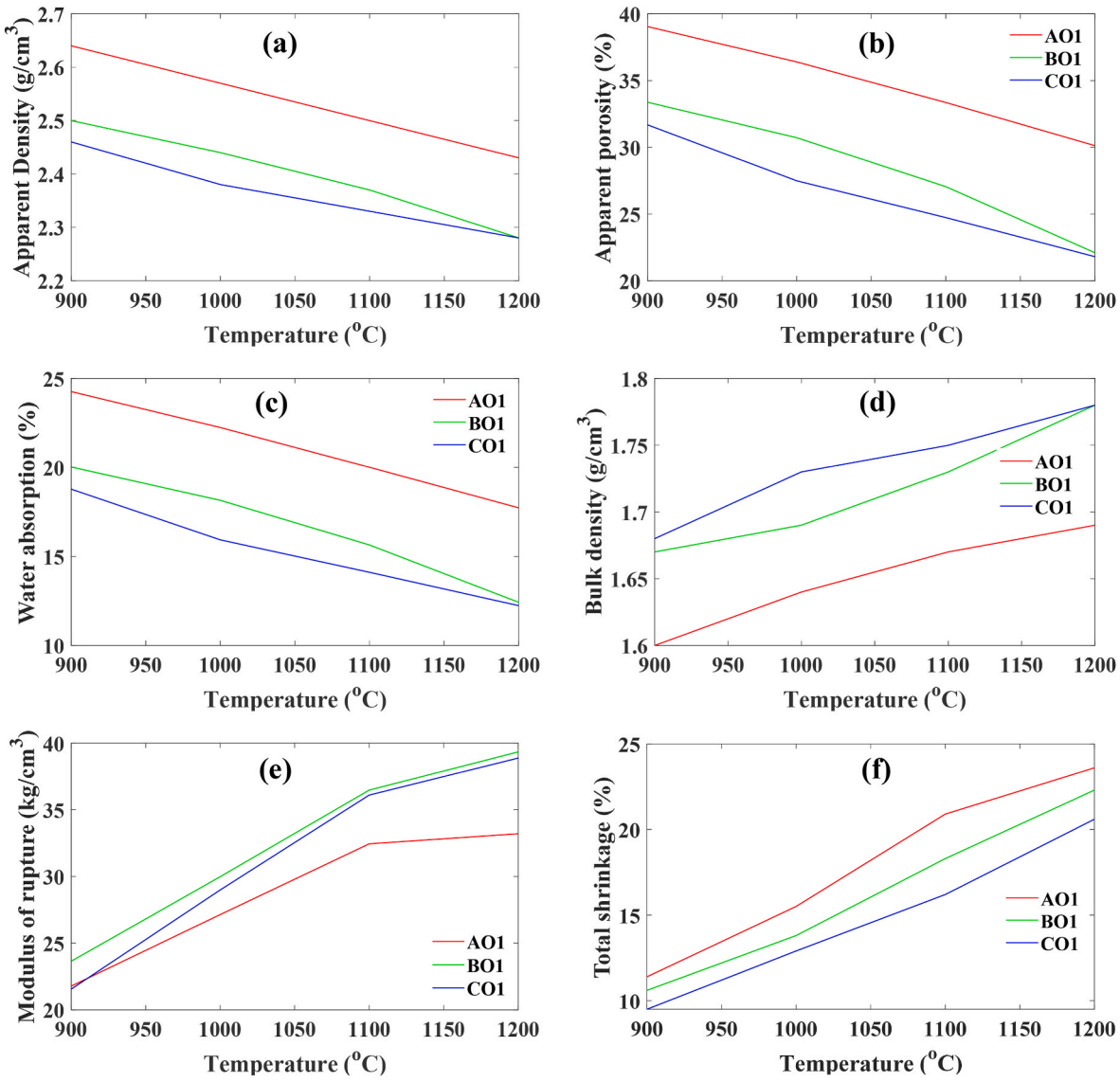

Fig. 1. Comparison of the physical properties of fired composites for different firing temperatures; (a) apparent density, (b) apparent porosity, (c) water absorption (d) bulk density, and (e) modulus of rupture (f) total shrinkage.

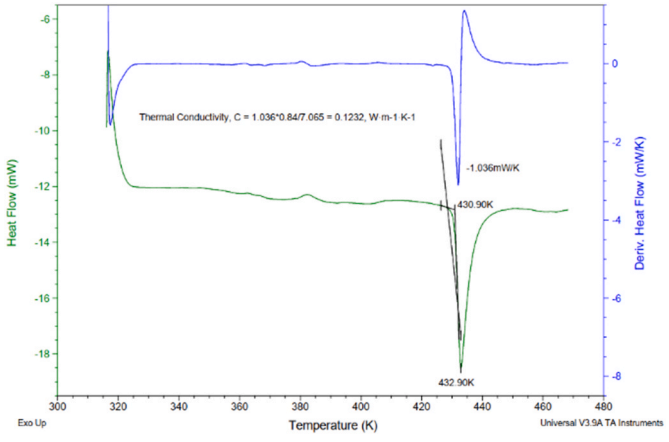

Fig. 2. DSC of neat Okitipupa clay.

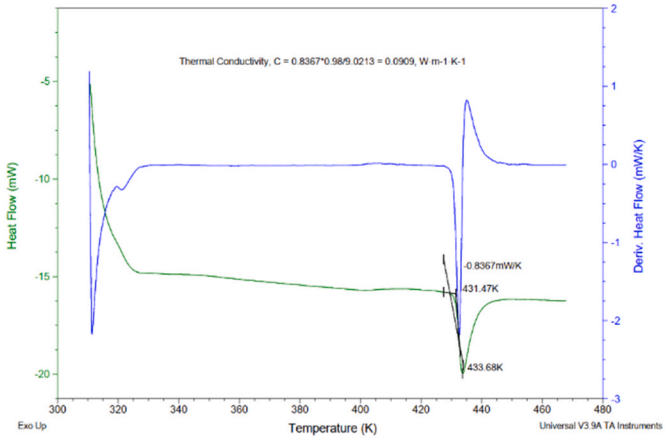

Fig. 3. DSC of 50 % clay, 30 % feldspar, 20 % silica.

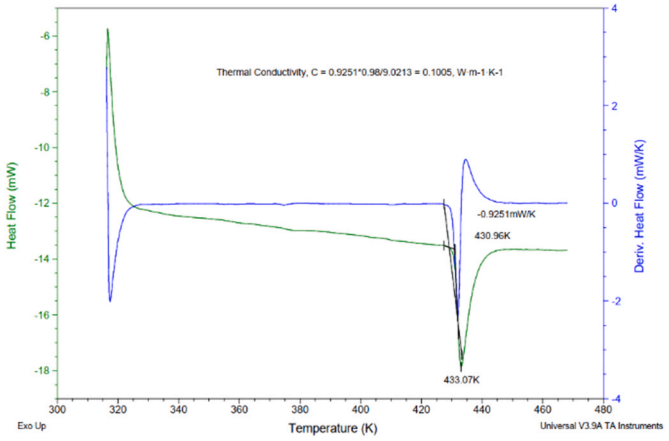

Fig. 4. DSC of 50 % clay, 25 % feldspar, 25 % quartz.

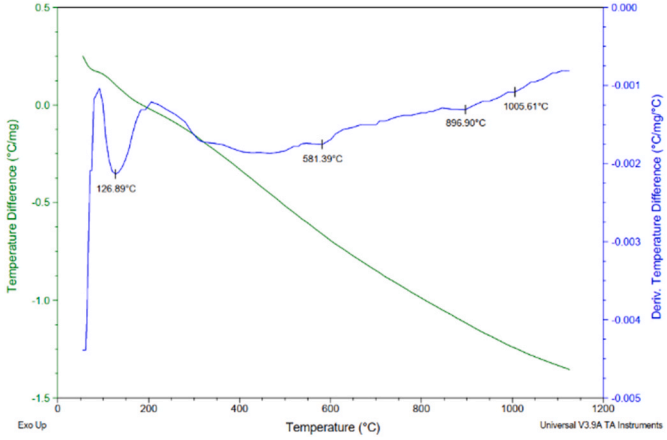

Fig. 6. DTA of 50 % clay/30 % feldspar/20 % quartz.

thermally stable and can withstand temperature fluctuations.

The derivative heat flow curves indicate a constant rate of degradation between 330 °C to 430 °C before the peak. There appears to be no difference in the reinforced and the unreinforced materials which implies that the effect of the reinforcement is not felt in the thermal stability characteristics of the clay sample. The rate of heating and the heat flow profiles for the three DSC thermograms corroborate the fact that the clay studied is thermal stable with or without the feldspar and quartz reinforcement.

The TGA measures the weight change as a function of temperature in the scanning mode or as a function of time in the isothermal mode in a controlled atmosphere [14]. The thermal stability curve of the raw clay is displayed in Fig. 5. The principal events from the thermographs affirm what was discussed in the DSC thermographs. The clay undergoes thermal degradation with a total weight loss of about 0.13 %. When subjected to a furnace temperature between 30 and 1000 °C, the initial loss was insignificantly low. The thermogravimetric analysis affirmed the fact that the clay analyzed is indeed thermally stable and that the processed materials were free from e impurities. This further confirms the applicability of this clay in structural industry.

The differential thermal analysis (DTA) thermographs in Figs. 6 and 7 indicate that no significant weight loss took place beyond 250 °C. As decomposition advances with a notable rise in temperature, more materials get degraded leading to insignificant weight loss. Between step one and step two, only about 0.041 mg representing less than 1 % of the material analyzed was lost. However, at higher temperatures (between 350 °C and 650 °C), there was a slight increase in the amount of decomposition. Again, this was insignificant compared to the amount of

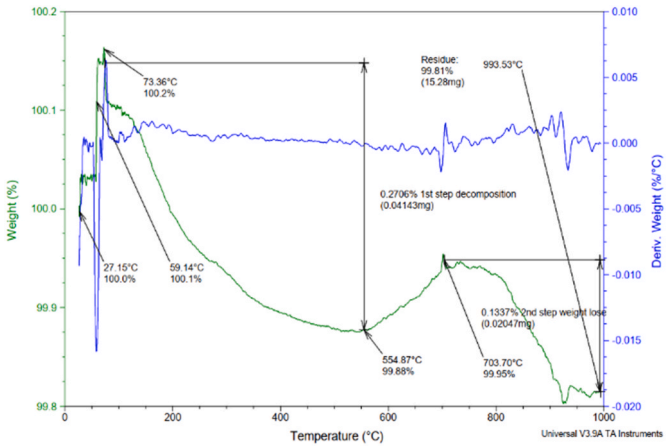

Fig. 5. TGA/DTG thermograph for raw clay.

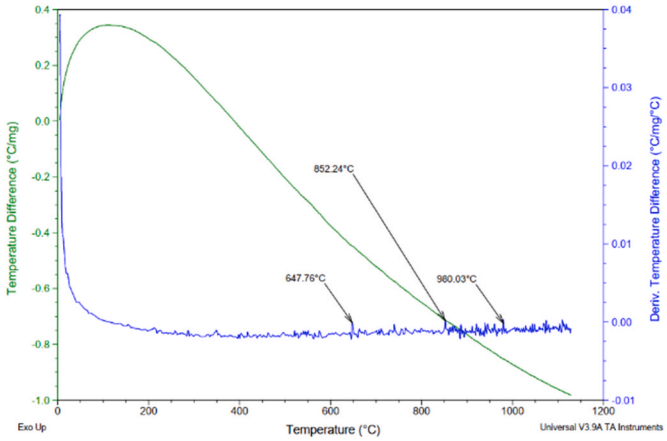

Fig. 7. DTA of 50 % clay/25 % feldspar/25 % quartz.

weight loss in the first step and other material types [26–28]. The material appears to have been completely stabilized after this stage as the amount of residue remained 99 % of the initial amount between 650 °C and 995 °C. This observation is similar to the derivative temperature difference profile shown in Figs. 6 and 7.

3.4. Microstructure analysis

The X-ray diffraction (XRD) patterns of the fired clay and fired composites were measured to identify the major clay and non-clay minerals such as kaolinite, albite, quartz, and orthoclase present in the

Table 3
XRD quantitative phase analysis of Okitipupa clay.

Minerals name	Formula	PDF #			Quantity (%)		
		AO1	BO1	CO1	AO1	BO1	CO1
Quartz	SiO_2	01-085-0865	04-015-8431	00-002-0471	52	44	42
Kaolinite	$Al_2Si_2O_5(OH)_4$	00-058-2004	00-058-2028	00-003-0052	33	37	18
Orthoclase	Al_2O_3. $K2O{\cdot}6SiO_2$	00-002-0475	00-002-0534	00-002-0534	8.3	11	32
Albite	$NaAlSi_3O_8$	00-003-0451	00-003-0451	00-003-0451	6	7.6	8

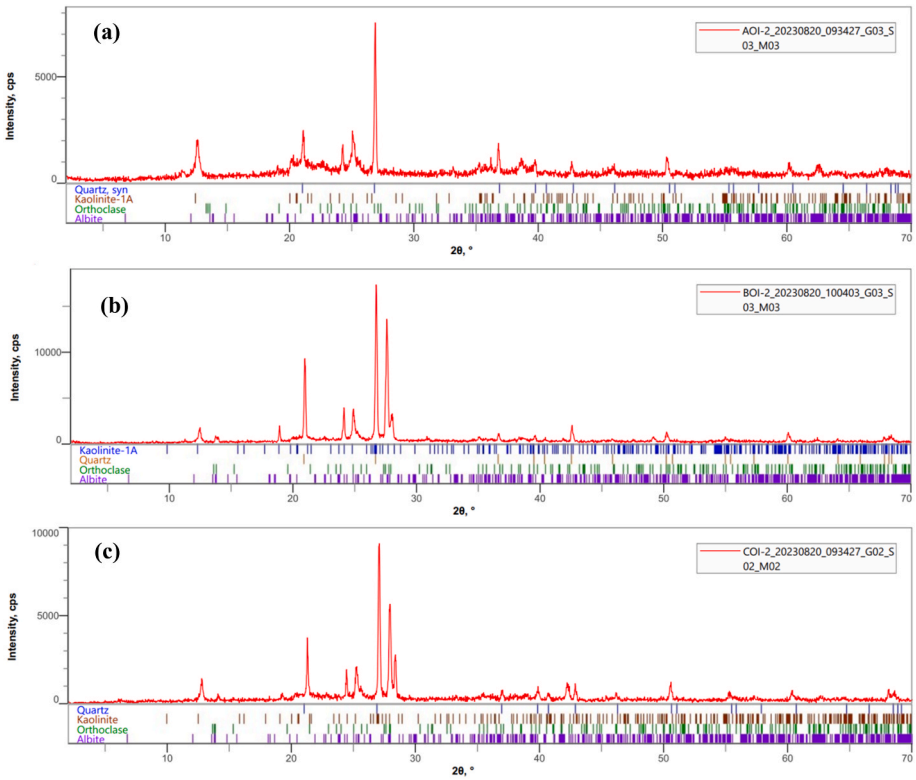

Fig. 8. XRD patterns of Okitipupa clay (a) AO1: 100 % clay, (b) BO1: 50 % clay, 30 % feldspar, 20 % quartz, (c) CO1: 50 % clay, 25 % feldspar, 25 % quartz.

bulk samples. The composition of these major phases is presented in Table 3 showing quartz (SiO_2) content the highest for each of the bulk samples peak at 27.5° (2θ) angle (Fig. 8). While albite ($NaAlSi_3O_8$) presents the lowest non-clay mineral content. Shan et al. [13] commented on the complexity of mineral compositions of natural clay and the challenges associated with controlling them artificially. Hence, the difficulty in investigating the influence of mineral content on the dynamic properties of clay. The authors also reported that although the plasticity index plays a significant role in the investigation of the dynamic properties of natural clay, variations occasioned by strong and/or loose absorbed water are primarily important indicators of the plasticity index in practical engineering. Therefore, the interrelationship between clay and non-clay minerals determines the overall properties that eventually dictate the application of the materials.

Generally, clay minerals are mainly small grains while the large grain size populations as illustrated in the SEM images (Fig. 9) are non-clay minerals [29]; the latter being from quartz. The SEM images presented imply that the bulk materials contain a substantial amount of large quartz grains. The high percentage of quartz in all the clay samples is responsible for the patterns seen in the XRD (Fig. 8) and the distribution in SEM images. The higher clay content promotes the bonding behavior between clay and non-clay minerals, thus, favoring improved mechanical strength of the bulk clay sample as observed in Fig. 1. This is in agreement with results obtained from similar studies reported in the past [30–32].

4. Conclusion

Quartz and feldspar-blended clay composites represent a paradigm shift in material science, apparently offering unparalleled thermal efficiency and structural performance. In this study, clay samples blended with quartz and feldspar were investigated to determine their potential areas of application. Investigation of the physical properties of the three different categories of bulk clay studied confirmed their suitability in the

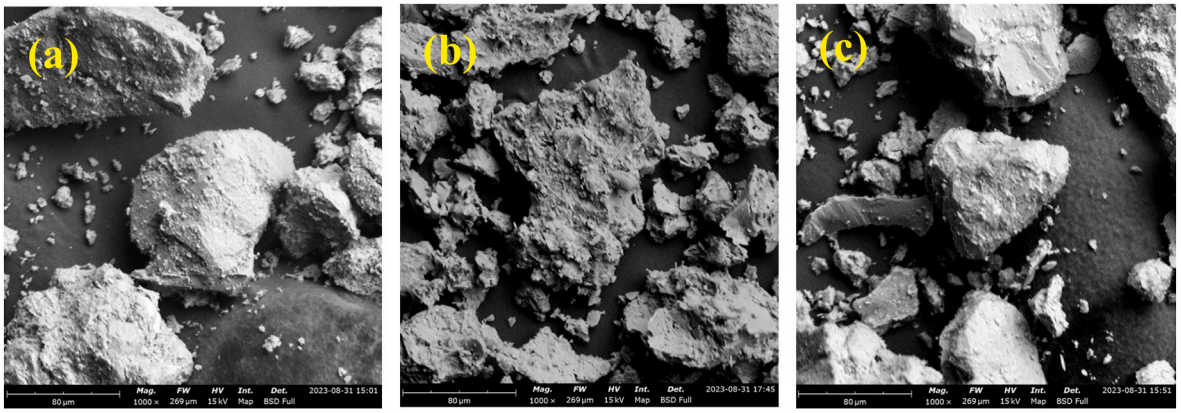

Fig. 9. SEM images of the specimens (a) AO1 (b) BO1 (c) CO1 after sintering at 1200 °C.

built environment, as well as other structural applications. Findings from this study further revealed that at the same temperature, the bulk density (1.69, g/cm^3, 1.78, g/cm^3, 1.78 g/cm^3), modulus of rupture (33.2 kg/cm^3, 39.34 kg/cm^3, 38.88 kg/cm^3), and total shrinkage (23.6 %, 22.3 %, 20.6 %) were at maximum. In addition, the results revealed that the relative plasticity of the clay samples improved with the addition of feldspar and quartz from 1.27 to 1.33 and 1.35 for the blended samples (BO1: 50 % clay, 30 % feldspar, 20 % quartz, and CO1: 50 % clay, 25 % feldspar, 25 % quartz), respectively. The clay used in this study has low iron content, and this contributes significantly to the reduction of gas formation at high processing temperatures. This study confirms that the addition of feldspar and quartz improves the plastic properties of the materials for manufacturing purposes. The improved plastic behavior of the blended clay samples enhances its formability, thereby leading to higher product quality and reduced manufacturing costs. Finally, the results of the microstructural analysis revealed a homogeneous distribution of the constituent parts of the bulk support, as well as the physical and mechanical stability of the materials. The high thermal stability of the clay increases the spectra of possible areas of application as the clay shows a high level of purity with high residue content after hydrolysis at 1200 °C. Future studies may consider investigating this clay sample for electrical insulation capacity for domestic electricity distribution and electric vehicles.

CRediT authorship contribution statement

Chijioke P. Egole: Writing – original draft, Formal analysis, Data curation. **Rasaq O. Medupin:** Writing – review & editing, Methodology, Conceptualization. **Gaius C. Nzebuka:** Methodology, Investigation. **Nnamdi A. Nnodum:** Formal analysis, Data curation. **Ugochukwu P. Ochieze:** Methodology, Investigation, Formal analysis. **Orevaoghene Eterigho-Ikelegbe:** Visualization, Formal analysis, Data curation. **Uwemedimo N. Wilson:** Writing – review & editing, Investigation. **Kelvin O. Yoro:** Writing – review & editing, Writing – original draft, Data curation.

Declaration of competing interest

The authors declare that they have no known competing financial interests or personal relationships that could have appeared to influence the work reported in this paper.

Data availability

Data will be made available on request.

Acknowledgments

The corresponding author is grateful to Lawrence Berkeley National Laboratory (LBNL) for funding the open acess publication of this paper.

References

[1] Y.L. Shuaib-Babata, S.S. Yaru, S. Abdulkareem, Y.O. Busari, I.O. Ambali, K.S. Ajao, G.A. Mohammed, Characterization of Baruten local government area of Kwara state (Nigeria) fireclays as suitable refractory materials, Nigerian J. Technol. 37 (2) (2018) 374–386. https://doi:10.4314/njt.v37i2.12.

[2] F.O. Aramide, K.K. Alaneme, P.A. Olubambi, J.O. Borode, Characterization of some clay deposits in South West Nigeria, leonardo elect, J. Pract. & Technol. 25 (2014) 46–57.

[3] A. Mucke, T.A. Badejoko, S.O. Akande, Petrographic-microchemical studies and origin of the Agbaja Phanerozoic Ironstone Formation, Nupe Basin, Nigeria: a product of a ferruginized ooidal kaolin precursor not identical to the Minette-type, Miner. Deposita 34 (1999) 284–296.

[4] M.M. Dansarai, M.A. Bawa, A. Tokan, Nigerian clay deposits for use as refractory materials in metallurgical industries - a review, Int. J. Eng. Res. Technol. 9 (6) (2020) 707–711.

[5] J.C. Ugwuoke, N.I. Amalu, Characterization of Obe clay deposits for refractory production, Amer. J. Eng. Res. 6 (12) (2016) 74–77.

[6] G.P. Ojo, U.G. Igbokwe, C.J. Egbuachor, K.K. Nwozor, Geotechnical properties and geochemical composition of kaolin deposits in parts of ifon, southwestern Nigeria, Amer. J. Eng. Res (AJER) 3 (6) (2017) 15–24.

[7] J.A. Amkpa, N.A. Badarulzaman, A.B. Aramjat, Influence of sintering temperatures on physico-mechanical properties and microstructure of refractory fireclay bricks, Int. J. Eng. Res. Technol. 8 (6) (2016) 2588–2593, https://doi.org/10.21817/ijet/2016/v8i6/160806214.

[8] I.T. Ojonimi, O. Aponbiede, F. Asuke, Geochemical and refractory properties of Egbahieme clay in Kogi state Nigeria, J. Raw Mater. Res. 147 (2016) 11–40.

[9] A.J. Ajala, N.A. Badarulzaman, Performance assessment of physico-mechanical properties of Aloji fireclay brick, Int. J. Integrated Eng. 8 (2) (2016) 13–15.

[10] C.O. Okpanachi, S. Sadiq, H.Z. Abdullahi, S.I. Ibrahim, V.C. Ezika, E.N. Yisa, G. O. Agada, Performance assessment of the physical properties of Kadna, Jagwai, and Gbakoita clay deposits as refractory for surface lining, Int. Innov. Sci., Eng. Technol. 4 (7) (2017) 2348–7968.

[11] P. Badica, A. Alexandra-Dinu, M.A. Grigoroscuta, A. Burdusel, V. Kuncser, M. Enculescu, C. Locovei, I. Porosnicu, I. Tiseanu, M. Ferbinteanu, I. Savulescu, M. Negru, N.D. Batalu, Mud and burnt roman bricks from romula, Scient. Rep. 12 (2022) 15864, https://doi.org/10.1038/s41598-022-19427-7.

[12] B. Kostova, B. Dumanov, K. Mihaylova, Archaeological bricks and tiles from southeast Bulgaria- determination of raw material and production technology by chemical, phase, and thermal analyses, Mediter. Archaeology and Archaeometry 23 (2) (2023) 1–22.

[13] Y. Shan, X. Wang, J. Cui, H. Mo, Y. Li, Effects of clay mineral composition on the dynamic properties and fabric of artificial marine clay, J. Mar. Sci. Eng. 9 (2021) 1216, https://doi.org/10.3390/jmse9111216.

[14] R.O. Medupin, O.K. Abubakre, A.S. Abdulkareem, R.A. Muriana, I. Kariim, S. O. Bada, Thermal and physico-mechanical stability of recycled high-density polyethylene reinforced with oil palm fibers, Eng. Sci. & Technol., an Int. Journal 20 (6) (2017) 1623–1631, https://doi.org/10.1016/j.jestch.2017.12.005.

[15] P. Chindaprasirt, A. Srisuwan, C. Saengthong, S. Lawanwadeekul, Synergistic effect of fly ash and glass cullet additive on properties of fire clay bricks, J. Build. Eng. 44 (June) (2021) 102942, https://doi.org/10.1016/j.jobe.2021.102942.

[16] A.O. Aluko, C.O. Ikubuwaje, Effects of grog additions on some refractory properties of raw (Abusoro) kaolin clay deposit for furnace lining, Adv. in Res. 21 (9) (2020) 180–191, https://doi.org/10.9734/AIR/2020/v21i930245.

[17] A. Samad, S. Baidya, U.S. Akhtar, K.S. Ahmed, S.C. Roy, S. Islam, Manufacture of refractory brick from locally available red clay blended with white Portland cement and its performance evaluation, Int. J. GEOMATE 20 (80) (2021) 105–112. https://doi:10.21660/2021.80.j2033.

[18] M. Ozonoh, T.C. Aniokete, B.O. Oboirien, B.C. Udeh, K.O. Yoro, M.O. Daramola, Prediction of emissions and profits from a biomass, tyre, and coal fired co-gasification CHP plant using artificial neural network: Nigerian and South African perspectives, in: J Phys Conf Ser, IOP Publishing, 2019 022021.

[19] B.P. Kagonbe, D. Tsozue, A.N. Nzeukou, S. Ngos, Mineralogical, geochemical and physic-chemical characterization of clay raw materials from three clay deposits in Northern Cameroon, J. Geosci. & Env. Prot. 9 (2021) 86–99. https://doi:10.4236/gep.2021.96005.

[20] M. Garcia-Valles, P. Alfonso, S. Martínez, N. Roca, Mineralogical and thermal characterization of kaolinitic clays from Terra Alta (Catalonia, Spain), Minerals 10 (142) (2020), https://doi.org/10.3390/min10020142.

[21] S. Mkaouar, W. Maherzi, P. Pizzette, H. Zaitan, M. Benzina, A comparative study of natural Tunisian clay types in the formulation of compacted earth blocks, J. Afr. Earth Sci. 160 (2019) 103920, https://doi.org/10.1016/j.jafrearsrsci.2019.103620.

[22] A. Merga, H.C.A. Murthy, E. Amare, K. Ahmed, E. Bekele, Fabrication of electrical porcelain insulator from ceramic raw materials of Oromia region, Ethiopia, Heliyon 5 (8) (2019) e02327, https://doi.org/10.1016/j.heliyon.2019.e02327.

[23] A. Merga Tullu, T.T. Terfasa, E.A. Zerfe, M. Tadese, E. Beyene, A.M. Abebe, D. M. Adoshe, Effect of cullet on firing temperature and dielectric properties of porcelain insulator, Heliyon 8 (2) (2022) e08922, https://doi.org/10.1016/j.heliyon.2022.e08922.

[24] J. Gao, W. Su, X. Wang, X. Song, J. Wang, J. Yang, G. Yu, Corrosion and degradation mechanisms of high chromia refractory bricks in an entrained-flow gasifier: experimental and numerical analysis, J. Mater. Res. Technol. 24 (2023) 8754–8765, https://doi.org/10.1016/j.jmrt.2023.05.120.

[25] M. Sawadogo, M. Seynou, L. Zerbo, B. Sorgho, G. Laure Lecomte-Nana, P. Blanchart, R. Ouédraogo, Formulation of clay refractory bricks: influence of the nature of chamotte and the alumina content in the clay, Adv. in Mater. 9 (4) (2020) 59, https://doi.org/10.11648/j.am.20200904.11.

[26] R.O. Medupin, O.K. Abubakre, A.S. Abdulkareem, R.A. Muriana, A. S. Abdulrahman, Carbon nanotube reinforced natural rubber nanocomposite for anthropomorphic prosthetic foot purpose, Scient. Rep. 9 (1) (2019), https://doi.org/10.1038/s41598-019-56778-0.

[27] O.K. Abubakre, R.O. Medupin, I.B. Akintunde, O.J. Tijani, A.S. Abdulkareem, R. A. Muriana, J.A. James, K.O. UkobaT-Cjen, K.O. Yoro, Carbon nanotube-reinforced polymer nanocomposites for sustainable biomedical applications: a review, J. Sci.: Adv. Mater. & Dev. 8 (2) (2023) 100557, https://doi.org/10.1016/j.jsamd.2023.100557.

[28] R.O. Medupin, O.K. Abubakre, A.S. Abdulkareem, R.A. Muriana, S.A. Lawal, Dimensional and thermal reliability of multi-walled carbon nanotube filled natural rubber nanocomposites, Int. J. Eng. Res. Afr. 51 (2020) 177–189, https://doi.org/10.4028/www.scientific.net/jera.51.177.

[29] M. Sawadogo, M. Seynou, L. Zerbo, B. Sorgho, G. Laure Lecomte-Nana, P. Blanchart, R. Ouédraogo, Formulation of clay refractory bricks: influence of the nature of chamotte and the alumina content in the clay, Adv. Mater. 9 (4) (2020) 59–67, https://doi.org/10.11648/j.am.20200904.11.

[30] F. Rosner, D. Papadias, K. Brooks, K. Yoro, R. Ahluwalia, T. Autrey, H. Breunig, Green steel: design and cost analysis of hydrogen-based direct iron reduction, Energy Environ. Sci. 16 (10) (2023) 4121–4134.
[31] L.I. Obidike, K.O. Yoro, Effect of zeolitic nano-catalyst on biodiesel yield and biochar formation during the pyrolysis of tallow, Biofuels 13 (6) (2022) 683–692.
[32] O.O. Sadare, M. Masitha, K.O. Yoro, M.O. Daramola, Removal of sulfur (eg DBT) from Petroleum distillates using activated carbon in a continuous packed-bed adsorption column, in: Proceedings of the World Congress on Engineering and Computer Science Vol. 2, 2018.